Desalination and Water Treatment
www.deswater.com
doi: 10.5004/dwt.2021.27759

238 (2021) 53–66
October

Characteristics of dissolved organic matter in surface water and fouling mechanisms during the ultrafiltration

Guizhen Feng*, Lin Huang, Yin Yang

School of Civil Engineering and Architecture, East China Jiaotong University, Nanchang, Jiangxi 330013, China, Tel. +13979119122; emails: 1491914560@qq.com (G. Feng), 2795905563@qq.com (L. Huang), sunnyyangyin@163.com (Y. Yang)

Received 8 February 2021; Accepted 26 August 2021

ABSTRACT

To learn about the characteristics of dissolved organic matters (DOM) in the surface water and identify the main foulants during the ultrafiltration (UF), the Ganjiang River was subjected to UF. Hydrophilicity and hydrophobicity, molecular weight distribution, and fluorescence characteristics of the surface water in the Ganjiang River were studied. Classification results showed that the DOM of the Ganjiang River was mainly hydrophobic (HPO) and a neutral hydrophilic fraction (N-HPI), which accounted for 40.06% and 29.69%, respectively. However, the proportions of transphilic (TPI) and charged hydrophilic fraction (C-HPI) were 18.91% and 11.33%, respectively. The fluorescence excitation-emission matrix illustrated that the Ganjiang River contained both humus-like organics and soluble microbial products with high response intensity and some protein-like organics which had weak response intensity. The membrane fouling test found HPO and N-HPI tended to cause a relatively large specific flux decrease, but a smaller degree of specific flux decline caused by TPI and C-HPI. The reversibility of membrane fouling revealed that HPO and N-HPI could easily cause irreversible fouling, while the TPI and C-HPI also contributed to irreversible fouling. The fitting results of the Hermia model indicated that standard blocking and cake filtration was the main membrane fouling mechanisms in the initial stage of filtration.

Keywords: Dissolved organic matter; Hydrophilic and hydrophobic property; Molecular weight distribution; Fluorescence characteristics; Membrane fouling mechanism

1. Introduction

Ultrafiltration (UF) has been regarded as one of the important water purification technologies and increasingly applied for water supply treatment recently due to its outstanding performance in particle, colloid and microorganism removal [1]. However, membrane fouling has always hindered the development of UF in water treatment. The prevention and mitigation of membrane fouling have been a hot topic in this field [2–8]. To alleviate membrane fouling, some strategies have been applied to the study of the mechanism of mitigating UF membrane fouling, such as ozone oxidation [1], powder carbon adsorption [6], and ultraviolet light oxidation [7]. For the different test subjects and conditions, the investigations that had led to the current mechanism of mitigating membrane fouling were still widely debated. Therefore, it is necessary to further study the mechanism of membrane fouling.

Recently, many researchers had pointed out that the fouling mechanism of natural organic matter (NOM) during the UF was the most essential [9,10]. Previous studies concluded that NOM was mainly composed of humic substances (such as humic acids, fulvic acids, humins), and non-humic substances (such as sugars, proteins, amino acids, esters, etc., accounting for about 20%–40% of the total amount of NOM) [11,12]. The molecular weight (MW) distribution, hydrophilicity and hydrophobicity,

* Corresponding author.

and fluorescence properties of NOM have an important influence on membrane fouling. When the above three characters were involved in previous findings, there were some different results and conclusions. In terms of MW distribution, the research by Tian et al. [13] showed that ultraviolet/persulfate (UV/PS) could reduce macromolecular organic matter in Songhua River (especially MW distribution: 5~30 kDa, >100 kDa), which could effectively alleviate membrane fouling; Li et al. [6] found that most of the organic matter (about 95%) caused by UF membrane fouling in Songhua River was a small and medium molecule organic matter, which MW was smaller than 30 kDa. In general, MW distribution was mainly related to steric hindrance, which in turn affects membrane fouling [1].

As for hydrophilicity and hydrophobicity, some controversies existed in previous studies. In early researches, hydrophobic organic compounds rich in aromatic carbon and carboxyl groups were considered to be the major membrane foulants [14–18]. Katsoufidou et al. [15] found that reducing the content of hydrophobic organic matter in water and increasing the content of hydrophilic organic compounds could mitigate membrane fouling. In recent years, hydrophilic fractions (such as polysaccharides and proteins) whose structure was rich in aliphatic carbon and hydroxyl groups gradually attracted the attention of membrane fouling researchers [5,8,19]. Although such substances were less in actual raw water, they might cause serious irreversible fouling. Yamamura et al.'s [8] research showed that the hydrophobic fractions did not increase membrane resistance, while the hydrophilic fractions caused severe loss of membrane permeability. Most research speculated that the effect of hydrophilicity on the fouling of UF could be related to the interaction force between the foulants and the membrane surface [20–23].

Fluorescence properties of dissolved organic matter (DOM) have received increasing attention in various natural water [4,7,19,22]. In these contexts, the fate of fluorescent natural organic matter (FNOM) was depicted during the UF. Some studies suggested that humus-like substances could cause initial membrane fouling, and when protein-like substances were enriched in the membrane surface, it determined membrane fouling behavior [19,24,25]. Other researchers thought that the synergistic fouling aggravated between the membrane and the FNOM [16]. At present, there is still no clear consensus on the contribution of FNOM fractions to membrane fouling. Therefore, it is important to study the fouling behavior of FNOM fractions for the prediction and controlling of the UF membrane fouling. At the same time, the Hermia model was the most widely used in the study of membrane fouling mechanisms [2,4]. Many studies had used this model to fit the membrane flux data to find the main membrane fouling mechanism [26,27]. In view of the foregoing, it is meaningful for mitigating membrane fouling to learn about the characteristics of major foulants and the main mechanism responsible for membrane fouling.

As the largest river in Jiangxi Province, the Ganjiang River is an important source of water for many water plants. Although UF is rarely used in water plants in this region, mastering the characteristic of DOM in the Ganjiang River and understanding the main membrane fouling mechanism will play an important role in promoting the development of UF. On the other hand, currently, most of the membrane fouling research was based on several simulated foulants, ignoring the comprehensive effects of various organic substances in natural water. Therefore, it is of great practical significance to carry out the membrane fouling test of natural water.

In this paper, the surface water of the Ganjiang River was used as the water samples to investigate characteristics of the DOM and the mechanisms of membrane fouling in particular: (1) the hydrophilicity and hydrophobicity, the MW distribution and the fluorescence properties of DOM; (2) the effect of hydrophilicity/hydrophobicity of DOM on membrane fouling and its removal; (3) identified the main membrane foulants by excitation-emission matrix (EEM) and attenuated total reflection Fourier-transform infrared spectrometer (ATR-FTIR) during the filtration; (4) based on the Hermia model to discuss the membrane fouling mechanism.

2. Materials and methods

2.1. Surface water

Surface water was collected from the Ganjiang River (located in Jiangxi Province of China). The main water qualities are summarized in Table 1. Due to the low content of DOM in the surface water, reverse osmosis (RO) was used to concentrate the dissolved organic carbon (DOC) into 20~30 mg L^{-1}. Then, the concentrated sample was filtered through the 0.45 μm membrane to remove the suspended particles and stored at 4°C in a refrigerator for subsequent use.

2.2. Membrane and UF experiment

A commercial flat sheet UF membrane (Snape Tech, Shanghai, China) with a molecular weight cut-off (MWCO) of 50 kDa was employed in this study, which was made of polyvinylidene fluoride (PVDF). An effective membrane area of this UF membrane was 38.5 cm^2. To remove impurities and achieve a stable permeate flux, all virgin membranes were pre-soaked in Milli-Q water for at least 48 h and stored at 4°C in a refrigerator for subsequent use.

All UF experiments were performed at room temperature (25°C ± 1°C). The UF unit can be found in Fig. 1. Dead-end flow experiments were undertaken using flat sheet, 90 mm diameter UF membranes in a stirred cell (SCM-300, Shanghai Institute of Applied Physics, China) with a constant transmembrane pressure (0.1 MPa) under nitrogen gas. The electronic balance (ME3002TE/02, Mettler Toledo, Switzerland) with data acquisition function measured the mass of the filtered solution every 10 s and recorded it into the computer. Prefiltration was conducted before membrane fouling using ultrapure water until a constant permeate flux (J_0) was achieved. A fresh membrane disk was used for each study. Every filtration experiment had two cycles, and 250 mL water samples were filtered in a cycle. At the end of the cycle, UF was backwashed with 50 mL of ultrapure water and 100 mL of ultrapure water was filtered to get a final flux (J_f) (Qu et al. [11]).

Table 1
The main water qualities of surface water

Parameters	pH	Turbidity (NTU)	Conductivity ($\mu S\ cm^{-1}$)	UV_{254} (cm^{-1})	Ca^{2+} ($mg\ L^{-1}$)	Mg^{2+} ($mg\ L^{-1}$)	DOC ($mg\ L^{-1}$)	SUVA ($L\ mg^{-1}\ m^{-1}$)
Values	6.56	21.22	120.1	0.2067	12.19	2.10	4.824	3.03

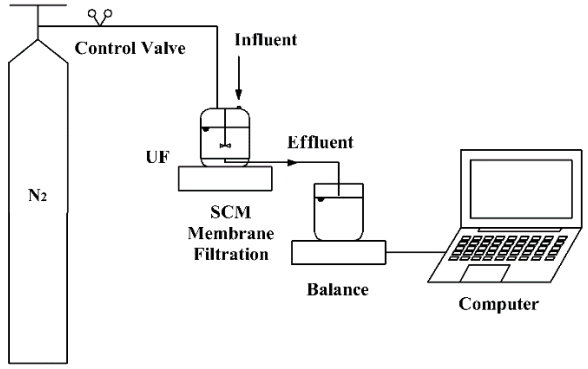

Fig. 1. Schematics of the membrane filtration setup.

2.3. Analytical methods

2.3.1. Ion exchange resin

In the test, Supelite DAX-8, Amberlite XAD-4 adsorption resin and anion exchange resin Amberlite IRA-958 produced by Sigma (USA) were used for the separation of hydrophilic and hydrophobic properties. According to Wong's method [28], the water samples after RO concentration were adjusted pH into 2 and filtered through DAX-8, XAD-4 and (after neutralization to pH 8) IRA-958 successively. Hydrophobic and hydrophilic substances were adsorbed on the resin. The remaining was considered as a neutral hydrophilic fraction (N-HPI). During elution, 0.1 M NaOH was used to elute the hydrophobic fractions from the DAX-8 and XAD-4 resins, the eluents were denoted as a hydrophobic fraction (HPO) and transphilic fraction (TPI), respectively; 1 M NaOH and 1 M NaCl were used to elute the negatively charged hydrophilic fraction (C-HPI), which adsorbed on IRA-958. Because pH influences the hydrophobicity of solution, prior to membrane fouling experiments, all the samples were neutralized to pH 7.0 and the DOC was adjusted to about 5 $mg\ L^{-1}$ with RO.

2.3.2. High-performance size-exclusion chromatography

Size exclusion chromatography with UV detection (SEC-UV_{254}) was be used to detect the apparent MW distribution of the sample waters after passing through a 0.45 μm membrane. Briefly introduced, a BIOSEP-SEC-S3000 column (Phenomenex, UK) (7.8 mm × 300 mm) was used to perform SEC and the mobile phase has adopted a solution of 10 mM sodium acetate (Aldrich, USA). Analysis using high-performance size exclusion chromatography was achieved by the high-performance liquid chromatography (Waters, USA) with a UV detector (2,489 UV detector, Waters) operated at 254 nm. The injection volume of water samples was 100 μL, and the flow rate was set at 1 mL min^{-1} [29]. To clear any residual and wash out the column of any contaminants, the mobile phase was purged at a volumetric flow rate of 2 mL min^{-1} before operation. The MW distribution pattern was derived by calibration with polystyrene sulfonate (PSS) MW standards of 1.37, 3.8, 6.71, 8.0, 8.6, 13.4 and 16.9 kDa [30].

2.3.3. Excitation-emission matrix

EEM was obtained using a fluorescence spectrometer (F-4500, Hitachi, Japan). Excitation wavelength (Ex): 220 ~ 450 nm, slit width: 5 nm, scanning interval: 10 nm; emission wavelength (Em): 250 ~ 550 nm, slit width: 5 nm, scanning interval: 10 nm, scanning speed was controlled to 1,200 nm/min. The water samples needed to be pre-treated with a 0.45 μm membrane and its pH was adjusted to 7.0 ± 0.1 before testing. The spectrum of Milli-Q water was recorded as the blank. Rayleigh and Raman scatter were eliminated through the interpolation method using Origin 2018 (OriginLab, Inc., USA). According to the research of Chen et al. [31], the EEM fluorescent region was divided into five regions, which represented different organic matters.

2.3.4. Other analytical methods

The DOC concentrations were determined using a Shimadzu TOC-L_{CPN} analyzer (Japan). Absorbance at 254 nm (UV_{254}) was measured by a UV-Visible spectrophotometer (UV759). $SUVA_{254}$ values were calculated by the ratio of UV_{254} to DOC. Turbidity was measured by a turbidity meter (2100P, Hach, USA); pH was measured by a PHS-25 pH meter; conductivity was measured by a lightning magnetic DDB-303A portable conductivity meter; zeta potential was measured with ZetaPlus (Brookhaven, USA). Functional groups on the surface of virgin and fouled membranes were examined using an attenuated total reflection Fourier-transform infrared spectrometer (ATR-FTIR, Spectrum Two, Perkin-Elmer, USA) to reduce the experimental error, all water quality indicators were measured in parallel three times, and the average value was taken.

2.4. Membrane fouling assessment

2.4.1. Membrane flux

Membrane flux can be calculated from Eq. (1):

$$J = \frac{V}{AT} \tag{1}$$

where V is the filtration volume (mL); J is the membrane flux ($m\ s^{-1}$); A is the effective area of the UF membrane

(3.32×10^{-3} m^2). Because membrane fouling is affected by many factors such as the membrane itself, the characteristics of the filtered water sample, and operating conditions, the specific flux (J/J_0) is usually used to describe the UF membrane fouling process, where J_0 is the pure water flux.

2.4.2. Membrane fouling reversibility

Membrane fouling that can be eliminated by hydraulic backwash is called reversible fouling (RF); otherwise, it is called irreversible fouling (IF); the sum of the two is called total fouling (TF). Philippe and Schaumann et al. [12] thought that reversible, irreversible and total membrane fouling can be quantitatively calculated with reference to Eqs. (2)–(4).

$$\mathrm{TF} = \frac{J_0 - J_f}{J_0} \tag{2}$$

$$\mathrm{IF} = \frac{J_0 - J_1}{J_0} \tag{3}$$

$$\mathrm{RF} = \mathrm{TF} - \mathrm{IF} \tag{4}$$

To investigate the total membrane fouling, a 250 mL water sample was filtered through the membrane. The final permeate flux was designated as J_f. TF can be calculated by Eq. (2). According to Qu et al. [11] methods to calculate IF and RF, the fouled membrane was backwashed by inverting the membrane in the cell and filtrating 50 mL ultrapure water. Then, the backwashed membrane was placed in its original orientation followed by 100 mL ultrapure water filtration. J_1 was the average permeating flux during filtrating 100 mL ultrapure water. IF and RF were calculated by Eqs. (3) and (4), respectively. Each filtration contains two cycles, which are called 1T and 2T, respectively.

2.4.3. Hermia membrane fouling model

The Hermia model is often used to describe the different membrane fouling stages of UF membranes. The models such as complete blocking; standard blocking; intermediate blocking; cake filtration. Based on the Hermia model, Shen et al. [32] used equations to describe the various pollution stages of the model, as shown in Table 2.

3. Results and discussion

3.1. Characteristics of DOM in the Ganjiang River

3.1.1. Hydrophilicity/hydrophobicity of DOM

The proportion of each fraction in the Ganjiang River (measured by DOC) is shown in Fig. 2a. It can be seen from Fig. 2a that there is a certain difference in the proportion of hydrophilic and hydrophobic organic matters in raw water. Among them, hydrophobic organic matter accounted for 58.97%, and hydrophilic fraction accounted for 41.02%. The proportion of each fraction is: HPO > N-HPI > TPI > C-HPI. It indicates that the Ganjiang River is dominated by HPO and N-HPI, while the content of TPI and C-HPI are relatively low, and the proportion of hydrophobic fraction is slightly higher than a hydrophilic fraction.

SUVA is defined as the UV of the unit organic carbon, which can be calculated from SUVA = UV_{254}/ DOC. It can reflect the degree of aromatic structure of organic matter, the larger the value, the higher the degree of aromatization [8,22,33]. What's more, it can also indirectly reflect the content of organic substances containing conjugated double bonds and benzene rings [33]. Fig. 2b shows that the SUVA of each fraction isolated from the surface water

Table 2
Hermia model

Models	Equations
Complete blocking	$J_0 - J = \mathrm{AV}$
Standard blocking	$1/t + B = J_0/V$
Intermediate blocking	$\ln J_0 - \ln J = \mathrm{CV}$
Cake filtration	$1/J - 1/J_0 = \mathrm{DV}$

J: flux; J_0: initial flux; V: filtration volume; t: filtration time; A, B, C and D are constants, respectively.

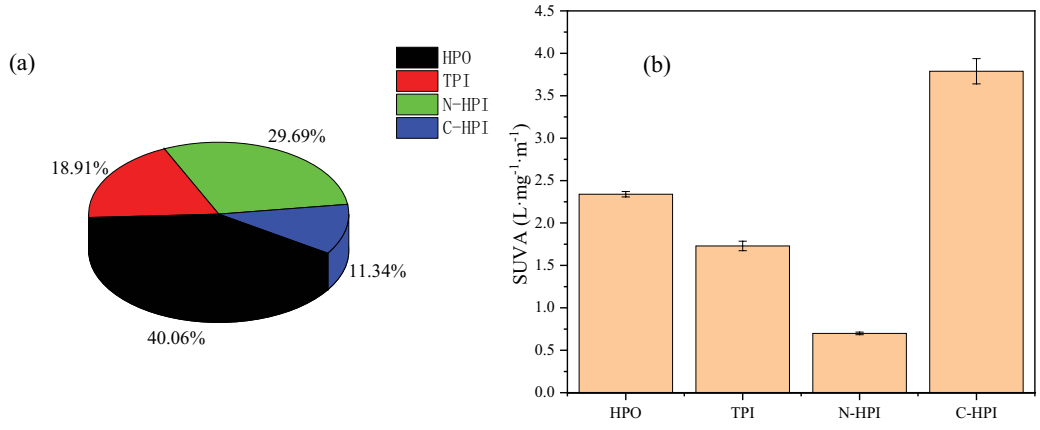

Fig. 2. (a) The proportion of each fraction in the Ganjiang River and (b) SUVA of four fractions.

of Ganjiang River. The relative magnitude of SUVA is: C-HPI [3.79 (L mg^{-1} m^{-1})] > HPO [2.34 (L mg^{-1} m^{-1})] > TPI [1.73 (L mg^{-1} m^{-1})] > N-HPI [0.70 (L mg^{-1} m^{-1})]. It is noteworthy that C-HPI has the highest SUVA. That is inconsistent with the previous study by Yamamura et al. [8]. They reported that the higher value of SUVA could imply more hydrophobic organic matter. Nonetheless, Wong et al.'s [28] research showed that C-HPI was mainly comprised of the protein organic matters, which contained a structure such as a benzene ring and could strongly absorb UV. This statement can support that why C-HPI owns the highest SUVA. As for hydrophobic fraction, maybe more unsaturated carbons (>C=C<) exist in HPO, leading to higher SUVA, and TPI contains more carbonyl carbons (>C=O), which will also increase its SUVA. N-HPI has the lowest SUVA, indicating that this fraction contains fewer organic compounds with characteristic structures such as conjugated double bonds and benzene rings, and this fraction may be mostly small molecular organic compounds [34].

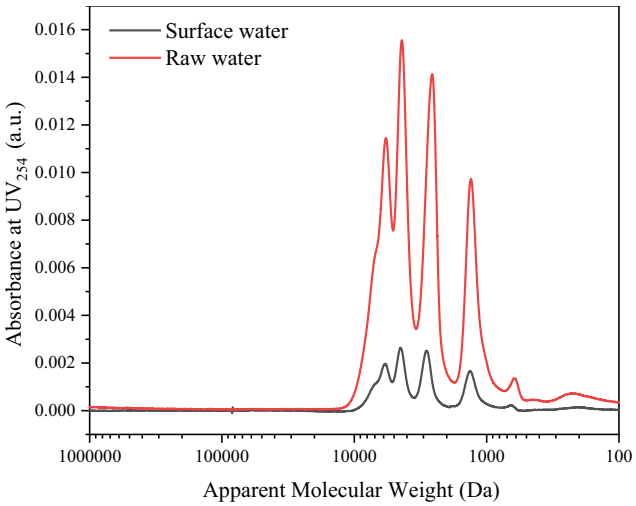

Fig. 3. MW distribution of surface water and raw water (through RO concentration).

3.1.2. MW distribution

Fig. 3 compares the MW distributions of surface water and raw water, in which the water sample diluted with total organic carbon to about 5 mg L^{-1} after RO concentration.

It can be seen from Fig. 3 that most peaks occur between 1 and 10 kDa. This suggests that the MW of DOM in the Ganjiang River is mainly medium MW (1 ~ 10 kDa), and most of this organic matter is composed of humic acid and other hydrophobic organic matters that have a strong response to UV [1,35]. The surface water of the Ganjiang River has basically no response to large MW (>100 kDa), and the response to small MW (<1,000 Da) is also very weak. On the one hand, this may be due to the low content of large MW and small MW organic matter in the surface water; On the other hand, it may be that the UV detector is not responding to some hydrophilic organic substances [35,36]. Yu et al. [1] investigated the MW distribution of organic matter in the Hyde park water and obtained similar results, but the medium MW organic matter was mainly distributed in 1,000~5,000 Da, which was smaller than that in this study. For raw water, the response intensity at small and medium MW increased significantly. This shows that by RO concentration, the content of medium and small MW organic matter has enhanced, while the content of large MW organic matter has basically remained unchanged. It further indicates that the DOM of the Ganjiang River is mostly dominated by medium MW organic matters, and also contains a small amount of small MW organic matters.

3.1.3. Fluorescence properties

According to the method of Qu et al. [11] for EEM fluorescence spectra, the EEM fluorescence spectra of the Ganjiang River were divided into five regions, as shown in Table 3. Simultaneously, combining the summary of fluorescence peak positions by Guo et al. [37], it is helpful to further understand the fluorescence properties of DOM reflected by EEM. EEM fluorescence spectra of raw water and four fractions are illustrated in Fig. 4.

As is shown in Fig. 4, the response regions of organic matter to fluorescence in raw water mainly appear in III and V. It is easy to discover the obvious peaks at Ex245/Em420 and Ex320/Em420, which can be named as peak A and peak C, respectively. These two peaks are attributed to humic-like substances such as fulvic acid and humic acid by previous reports [3,4,22,37]. As stated by Henderson et al. [38], the predominant fluorescence for clean reservoirs and rivers was normally peak A and peak C. Meanwhile, there is also a certain fluorescence peak T in the IV region, but it is relatively weaker than the intensities of peaks A and C. This indicts that in addition to the main humic acid and fulvic acid, there also contains some protein-like substances related to the metabolites of the soluble microorganisms in the raw water of the Ganjiang River. Liu et al. [22] also obtained a similar 3D fluorescence EEM of the Gaoyu Reservoir (GY), but there were some differences in Sanhaowu Lake (SHW) and Huangpujiang River (HPJ), which contained much more protein-like fluorophores. Because SHW water and HPJ water presented the heavier polluted than the GY water.

To further understand the main organic matters in each fraction after hydrophilic classification, this study continues to analyze the four fractions by EEM. As shown in Fig. 4, the HPO fraction has the highest fluorescence response intensities, while the other three fractions have comparable response intensities. At the same time, the response positions of the strongest fluorescence peaks in each fraction are different, indicating that there are differences in the types of organic matter in each fraction. In the HPO fraction, the strongest fluorescence peak appears in the transition region of the III and V regions, while in the TPI and C-HPI fractions, the strongest fluorescence peak appears in the III region. Comparatively, peak A which has different excitation and emission is dominant in the TPI fraction, it may explain that fulvic-like fluorophores are different from HPO and they are the richest in this fraction. It is worth noting that peak B and peak T in Em < 350 nm (the emission wavelength less than 350 nm)

Table 3
Fluorescence region of dissolved organic matter

Region	Excitation wavelength (nm)	Emission wavelength (nm)	Dissolved organic matter
I	<250	<330	Aromatic protein (tyrosine)
II	<250	250~380	Aromatic protein (tryptophan)
III	<250	>380	Fulvic acid-like
IV	>250	200~380	Soluble microbial by-product-like
V	>250	>380	Humic acid-like

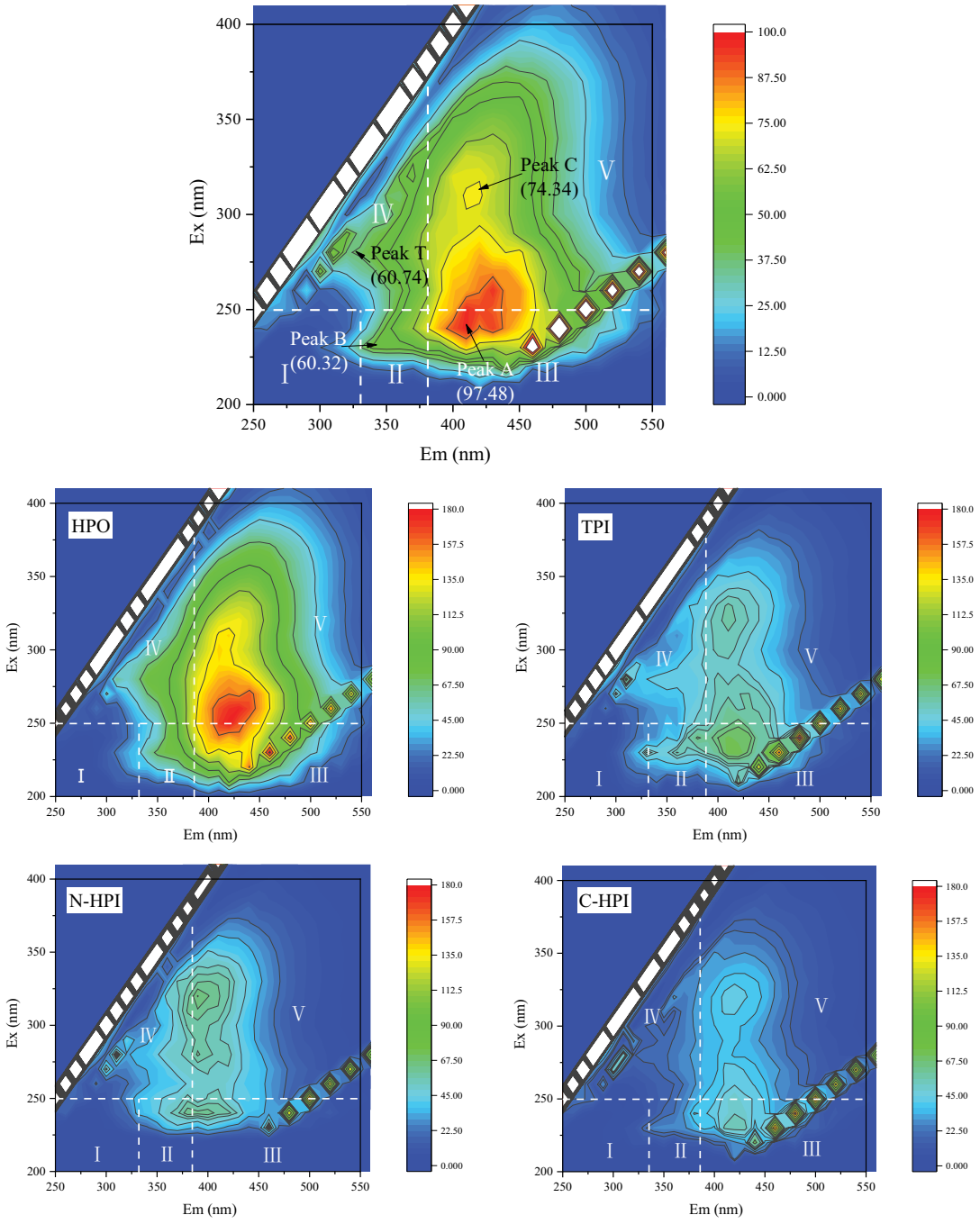

Fig. 4. EEM fluorescence spectra of raw water and four fractions (DOC ≈ 5.0 mg L^{-1}; pH = 7.0 ± 0.5; 25°C).

are obvious in the TPI fraction, which was associated with protein-like substances such as tryptophan and tyrosine [11,39]. Previous reports pointed that hydrophobic fractions have longer excitation and emission wavelengths than hydrophilic ones which were similar to this study [38–41]. Nonetheless, peak locations of fractions exist difference because of different classification methods of DOM.

Moreover, In the N-HPI fraction, the strongest fluorescence peak appears near the junction of the IV and V regions, which implies some protein-like organic matters related to microbial metabolism and some humic/fulvic-like organic matters that existed in this fraction. It is interesting to notice that the humic/fulvic-like fluorophores' locations are different from those in hydrophobic fractions. Compared with other fractions, the peak A and peak C's emission wavelengths in N-HPI fractions are shorter than others. Wu et al. [40] and Liu et al. [22] also observed a similar phenomenon in their research. Many previous studies try to explain this phenomenon. Zhang et al. [41] believed that the blue shift of the fluorescence peak position was related to the decrease in the number of aromatic rings and molecular weight of organic compounds; Swietlik et al. [42] showed that the reduction of polar groups (such as amino, hydroxyl, carboxyl, etc.) in water could also cause the blue shift of the fluorescence peak. That is to say, the large aromatic molecules' break-up or the decrease of aromatic rings in a chain structure may lead to the above phenomenon. Besides, Senesi [43] stated that the blue shift can also be caused by an elimination of particular functional groups such as carboxyl, hydroxyl and amine.

3.2. Membrane fouling and identification of major foulants

3.2.1. Specific flux

The flux decline with raw water and four fractions is shown in Fig. 5a. It can be observed that raw water and four fractions in flux behavior have a significant difference. Before the filtration volume comes about 110 mL, the flux of the HPO fraction drop most rapidly, followed by the N-HPI fraction, and the C-HPI fraction showed the least. When the filtration volume exceeded 110 mL, the flux declined quickly was raw water, followed by the N-HPI and HPO fractions, which had a similar flux decline. However, the TPI and C-HPI fractions always presented a slight flux decline. That is to say, both the HPO and N-HPI fractions contribute to fouling, but the TPI and C-HPI fractions for the fouling had a slight response. Additionally, for the second filtration cycle, each fraction had a more visible response to the flux decline. Since most of the membrane fouling caused by N-HPI was IF, backwashing could not remove IF, so the specific flux attenuation of 1T was higher than 2T. The relative magnitude of specific flux is: C-HPI > TPI > N-HPI > HPO. This result is consistent with a previous study on MF fouling potential by different DOM fractions [22,44]. It is interesting to note that, for raw water, there is no synergistic increase in fouling, while the N-HPI and HPO fractions decrease more seriously than the flux in the initial stage of each cycle. This may be due to the properties (such as molecular weight, hydrophobicity) of each fraction is more concentrated compare with the raw water, which will cause more serious membrane pore blockage at the beginning of filtration. It can also be found from Fig. 5a that the specific flux curve of raw water is obviously different from that of other fractions, and the end specific flux of the two cycles is the lowest, 0.76 and 0.63, respectively. It means that the membrane fouling caused by raw water is the most serious. According to the former researches, it can be attributed to the fact that raw water contains organic matter with different molecular weights and hydrophilic and hydrophobic properties. During the filtration, various fouling mechanisms such as adsorption, membrane pore blockage, electrostatic repulsion, hydrophobic force, and filter cake layer filtration could be induced [1,11,41,42,44].

Furthermore, previous studies had shown that the more hydrophobic organic matters, the larger MW; and the smaller MW, the stronger hydrophilicity, which implies the HPO fraction was composed of large MW organic matters [1,4].

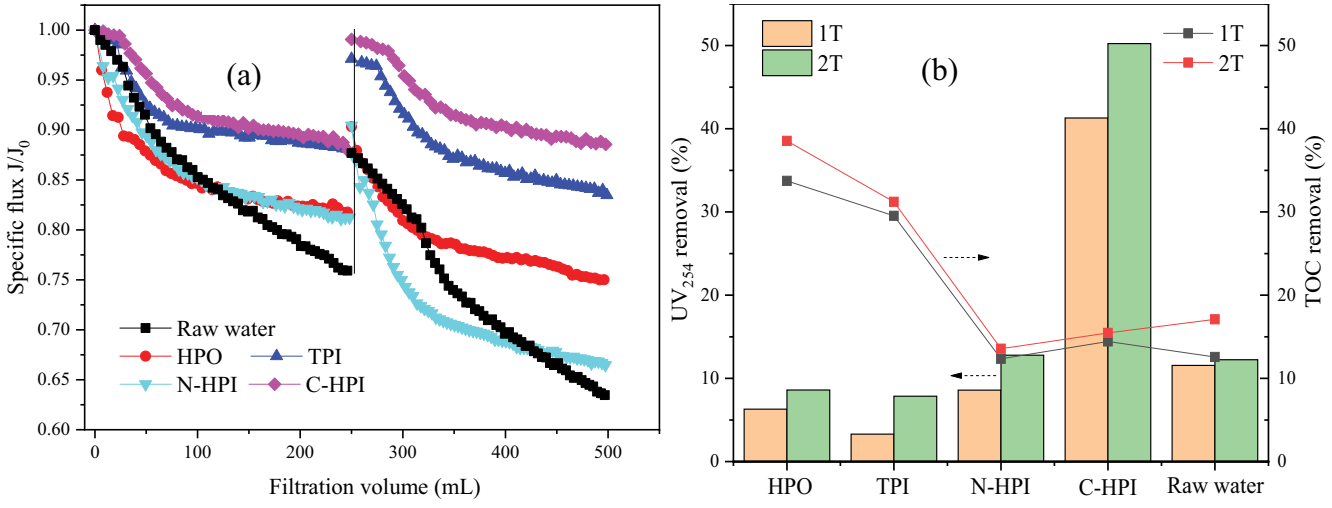

Fig. 5. (a) Flux decline of raw water and four fractions (DOC ≈ 5.0 mg L^{-1}; TMP = 0.1 MPa; pH = 7.0 ± 0.5; 25°C) and (b) removal of organic matter from four fractions and raw water (by UV_{254} and DOC).

At the same time, because the N-HPI fractions are mostly uncharged organics, they will not have electrostatic repulsion with the membrane surface or the filter cake layer, which makes it easier for organic matters to deposit on the membrane surface, causing a large number of membrane pores to be blocked, forming serious specific flux decline [41]. It can explain that the more pronounced decline in specific flux caused by the N-HPI and HPO fractions. On the other hand, the decrease in the specific flux of the TPI and C-HPI fractions in the two cycles is relatively slight, and the C-HPI fraction has the largest end specific flux value, which is 0.88. This may result that these two fractions are mostly small MW organics, which are not easy to deposit on the membrane surface and are more likely to pass directly through the membrane pores, and the C-HPI fraction contains polar functional groups, which is likely to cause electrostatic repulsion with the membrane surface, reducing the deposition of large MW organics on the membrane surface and the adsorption of small MW organics on the membrane pores [22,41,44].

3.2.2. Organic matter removal and membrane fouling reversibility

It is important for achieving drinking water quality to study the removal of organic matter during water treatment processes. Herein, the UV_{254} and DOC were used to investigate the different removal of organic matter by UF (Fig. 5b). It can be seen from Fig. 5b that the removal of DOC, the UF membrane was more inclined to trap hydrophobic fractions, especially the HPO fraction, and the highest removal rate is 38.54%. However, the DOC removal rates of the N-HPI fraction and the raw water were relatively low, which was inconsistent with the rapid decline of its membrane-specific flux. It can be inferred that there is no positive correlation between the removal of DOC and the fouling of organic matter to the membrane [8,45,46]. Maybe there is a small amount of biological macromolecular organic matter in the N-HPI fraction and raw water. It is sufficient to cause a serious decrease in membrane flux, while most small molecular substances can pass through the membrane pores. Yu et al. [1] also considered that biological macromolecular organic matters in natural raw water are the main substances that cause UF membrane fouling.

In terms of UV_{254} removal, the C-HPI fraction was the highest, reaching 50.24%, while the retention efficiency of other fractions was poor, their removal rates were about 10.00%. The UV_{254} removal rate of the TPI fraction was the lowest, which was 3.29%. This may be related to the bare absorbance at 254 nm of the hydrophilic fractions, such as polysaccharides and protein. Comparing the hydrophilic fractions, little organic matter in the hydrophobic fractions was removed by considering UV_{254} because of the undetectable absorbance of these fractions [4,47].

To determine the irreversible foulants that cause membrane fouling, this study further investigated the reversibility of membrane fouling as shown in Fig. 6. It can be noticed that the total relative fouling caused by raw water in the two filtration cycles is the largest, which was 0.24 and 0.37 respectively. Obviously, the lowest relative

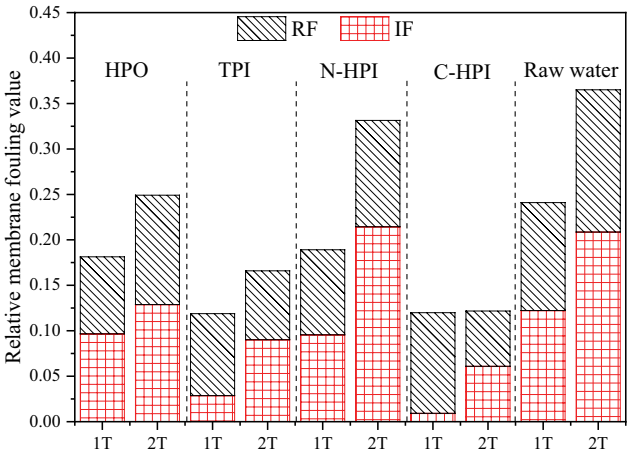

Fig. 6. Membrane fouling reversibility of fractions and raw water.

fouling value (0.12) was resulted from the C-HPI fraction. Comparing the irreversible fouling (IF) and reversible fouling (RF) among the four fractions and raw water, the IF was relatively higher in the HPO, N-HPI and fractions and raw water, which means these fractions may cause IF. This may be due to the fact that in the HPO fraction, small molecules of humic-like and fulvic-like organic matters were easily adsorbed on the membrane pores, while small molecule protein-like organics in the N-HPI fraction were more easily adsorbed on the inside of the membrane pores and were hard to hydraulically remove. Yamamura et al. [8] also found that the HPO and N-HPI fractions were the main foulants causing membrane fouling. According to their analysis, humic-like organics had a higher content in the HPO fraction, which were easily adsorbed in the membrane pores to narrow the membrane pores, or blocked the membrane pores by binding with other small molecules through hydrophobic interactions. Some protein-like substances metabolized by microorganisms in the N-HPI fraction were adsorbed on the membrane surface, forming irreversible fouling. Additionally, soluble Ca^{2+} and Mg^{2+} in water will change the surface potential of organic matter on the one hand and affect the electrostatic repulsion. On the other hand, it will also form complexes with organic matters, promoting the formation of zeta potential and larger colloids, and strengthen the pollution of UF membranes by protein-like and humic-like organic substances [31].

3.2.3. Subtraction EEM fluorescence spectra

To identify the main foulants trapped on the UF membrane, the subtraction method was used to compare the EEM fluorescence spectra of the fractions and raw water of the Ganjiang River before and after UF, as illustrated in Fig. 7.

The EEM difference chart of hydrophobic components (i.e., a, b) is significantly wider than that of hydrophilic components (i.e., c, d), and the fluorescence signals are denser in regions III and V, indicating that humic acids and fulvic acids are more likely to be trapped by UF membranes. This is mainly due to the fact that these organic matters while changing the properties of the membrane surface, will also strengthen the bridging effect of organic

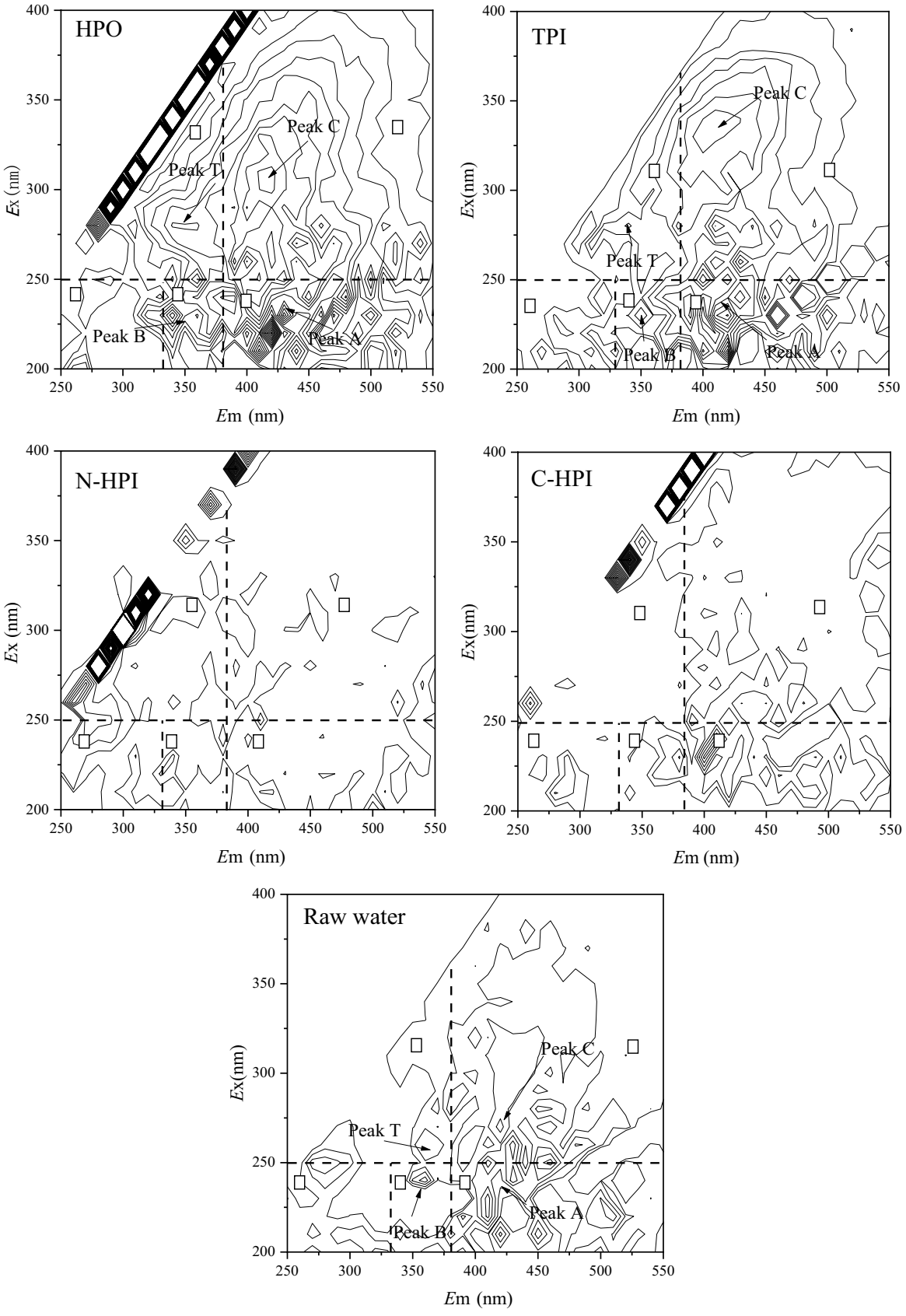

Fig. 7. Subtraction EEM fluorescence spectra of four fractions and raw water by UF.

matter and soluble inorganic ions on the membrane surface [3,48–50]. However, the specific flux of the N-HPI fraction decreased to a greater extent, which again shows that there is no positive correlation between the retention of organics and membrane fouling. Moreover, the fluorescence of the HPO fraction in the III–V region is denser than that of the TPI fraction, which indicates that after UF more organic matter is trapped in the HPO fraction. According to the previous researches [22,42,44], the reason for this result may be that the organics in the HPO fraction are mostly macromolecular humic acid and fulvic acid, while the molecular weights of the organics in the TPI fraction are smaller. Additionally, the retention of these two fractions in the IV region is similar, because the organics in this region are mostly small molecule soluble microbial products (SMPs), which are easily adsorbed inside the membrane pores to form irreversible membrane fouling [8,35].

Furthermore, the fluorescence signal reflected by the EEM subtraction chart of the N-HPI fraction is mainly concentrated in regions I, II and IV. It suggested that some SMPs and aromatic protein substances in this fraction were retained. Most previous studies had shown that SMPs and small-molecule protein-based organics were the main substances that constitute irreversible membrane fouling during the UF [1,8,13,18,51]. From the observation of the EEM subtraction chart of the C-HPI fraction, it is clearly observed that only a few small molecule proteins, humic acids and fulvic acids in regions I, III, and V were retained. When these DOM passed through the membrane pores, they would be adsorbed inside the membrane pores, which was difficult to recover by water washing, and it was easy to form irreversible membrane fouling.

Besides, it is found that the fraction of raw water has a certain degree of fluorescence in the V area. Combined with the analysis of the specific flux change curve, the reason why the specific flux of the raw water decreases so quickly is that the humic acid macromolecules in this fraction are deposited on the membrane surface, which causes effective membrane pore area on the membrane surface to decrease, thereby reducing its membrane flux. Yu et al. [1] and Yamamura et al. [8] considered that biological macromolecular organic compounds in raw water were the main substances that cause UF membrane fouling. At the same time, the raw water also has fluorescent regions in the areas I, III and IV, which indicates that it also contains some proteinaceous substances, SMP and fulvic acid substances, which will be adsorbed and deposited on the membrane pores or the membrane surface, further decreasing the membrane flux. This result is in agreement with the finding by Liu et al. [22] that the more the fluorophores existed in the fraction, the more serious membrane fouling could be achieved to the fraction.

3.2.4. Characterization of membrane surface

To further evaluate the foulants trapped on the surface of the UF membrane, ATR-FTIR was used to scan the surface of virgin and fouled membranes (Fig. 8).

Compared with the virgin membrane, UF membranes filtered through raw water and fractions have various degrees of absorbance peaks around 3,280; 2,930; 1,650; 1,537; 1,240 and 1,040 cm^{-1}. It was assigned to the stretching vibration of hydrogen bonds (O–H), which the absorbance band near 3,280 cm^{-1}. And the weak signal at 2,930 cm^{-1} was attributed to the C–H stretching vibrations [13,52]. They are typical functional groups of hydrophilic polysaccharides. It is obvious that the absorption intensities of the N-HPI and C-HPI fractions at 3,280 and 2,930 cm^{-1} were significantly stronger than those of the HPO and TPI fractions. That is to say, the more hydrophilic polysaccharides exist on the membrane surface, the more serious membrane fouling could be achieved to the hydrophilic fractions. Additionally, a previous study revealed that the stretches at 1,650 and 1,040 cm^{-1} were associated with the carboxylate group (COOH), implying that carbohydrate-like substances were retained in the fouling layer [13,52,53]. Moreover, deposition of protein-like organic matters could be found in the membrane surface fouled by the N-HPI and C-HPI fractions, which the characteristic groups of amino compounds (N–H) were observed at 1,537 cm^{-1} [13,54]. There is reasonable to find humic-like and protein-like substances in the fouling layer, according to the fluorescent EEM spectra.

3.3. Membrane fouling mechanism based on Hermia model

Hermia model, as mentioned in Table 2, was applied to further analysis of the raw water and four fractions fouling evolution (Table 4). It can be seen that the fitting degree of raw water to the Hermia model ($R^2 > 0.945$) is generally higher than the fitting degree of each fraction to the model ($R^2 > 0.712$). In each fraction, four classic filtration models all fit well to experiment data, among which the standard blocking model manifests the most excellent fitting. It could be referred that in the actual UF process, it was not a single membrane fouling mechanism at work, but multiple membrane fouling mechanisms that work together. Among these models, standard blocking and cake filtration are the dominant mechanisms of membrane

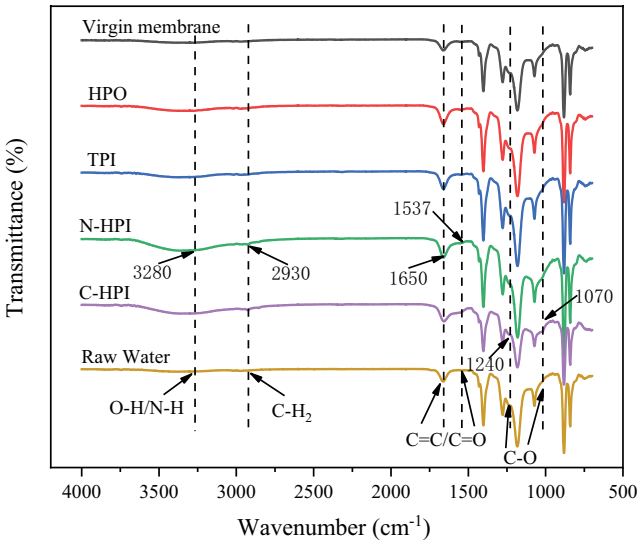

Fig. 8. Variation of Fourier-transform infrared spectra of virgin membrane and membrane of UF four fractions and raw water.

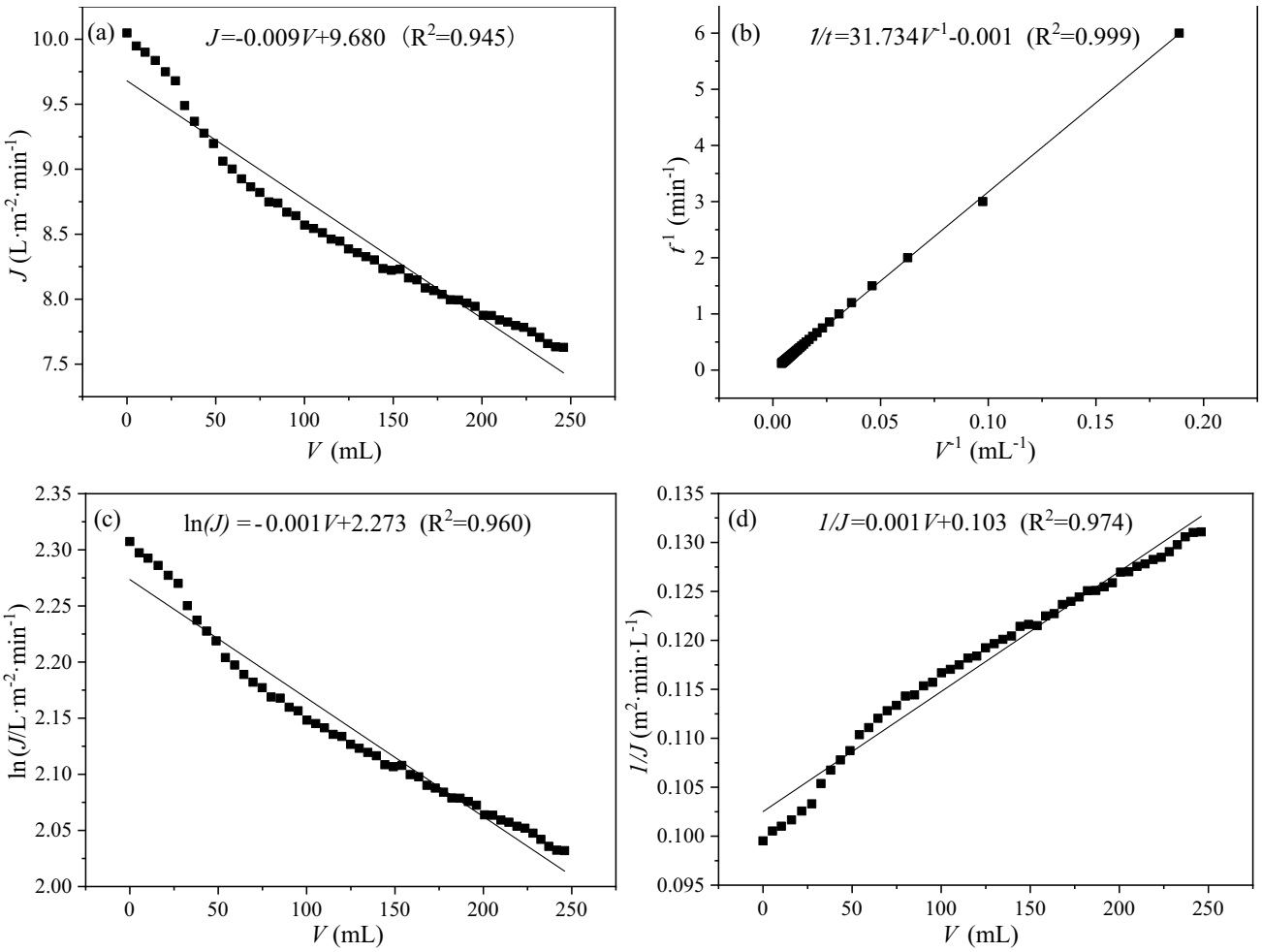

Fig. 9. Fitting of membrane fouling of raw water on Hermia model (a) complete blocking, (b) standard blocking, (c) intermediate blocking and (d) cake filtration.

fouling, taking R^2 as a measure of goodness of fit. Sun et al. [45,46], Wan et al. [4], and Shen et al. [32] also obtained similar findings. Moreover, the regression results of the raw water are given in Fig. 9. As shown, the R^2 values were 0.945, 0.999, 0.960, and 0.974 for complete blocking, standard blocking, intermediate blocking, and cake filtration, respectively, which implied that standard blocking and cake filtration dominated the membrane fouling, and the other two models were to some extent involved as well. Standard blocking can be ascribed to the DOM depositing on the pore walls, which leads the pore size to be narrowed. Shen et al. [32] found that complete blocking was the fouling mechanism of hydrophilic substances that was mainly attributed to complete. However, the result of this paper is consistent with Wan et al.'s studying [4]. Thus, there are some differences in previous researches may be due to the different samples.

Comparing the R^2 of the hydrophobic component and the hydrophilic component when passing through the membrane, it can be found that except for the N-HPI,

Table 4
Comparison of membrane fouling mechanism of raw water and various fractions through UF (R^2)

Fractions cycles fouling model	HPO		TPI		N-HPI		C-HPI		Raw water	
	1T	2T	1T	2T	1T	2T	1T	2T	1T	2T
Complete blocking	0.717	0.803	0.700	0.840	0.814	0.738	0.823	0.853	0.945	0.963
Standard blocking	0.996	0.999	0.985	0.999	0.975	0.999	0.982	0.999	0.999	0.999
Intermediate blocking	0.740	0.822	0.712	0.853	0.833	0.769	0.833	0.861	0.961	0.975
Cake filtration	0.762	0.840	0.725	0.866	0.851	0.800	0.843	0.869	0.974	0.985

the R^2 of other fractions increases with the extension of the filtration cycle. This may be due to the fact that the N-HPI was composed of mostly small molecular organic compounds, which are more likely to be adsorbed on the membrane pores, causing standard blocking; while other fractions also have organic substances close to or larger than the membrane pores, which continuous accumulation and adhesion on the membrane surface and membrane holes make it closer to each model. On the whole, the fitting conditions of the four types of models between the raw water and the fractions are as follows: standard blocking > cake filtration > intermediate blocking > complete blocking. It implies that in the initial stage of filtration, standard blocking is the main factor, and also considered that standard pore plugging to be the main mechanism of IF. With the progress of membrane filtration, cake filtration will become the dominant mechanism in the later stage of filtration, and filter cake layer filtration may cause the main factor of RF.

4. Conclusions

In this study, the characteristics of DOM in the natural raw water of the Ganjiang River and the fouling mechanisms during UF were investigated. The following conclusions can be drawn:

- The Ganjiang River was mainly HPO and N-HPI organic matters, which accounted for 40.06% and 29.69% respectively, TPI and C-HPI had relatively small proportions, 18.91% and 11.33%, respectively. It can be known from SUVA that the aromatics and organic compounds containing unsaturated characteristic bonds such as benzene rings and conjugated double bonds were mostly presented in the HPO and C-HPI fractions, while the TPI and N-HPI fractions were less.
- The DOM of the Ganjiang River was mostly humic-like and fulvic-like substances, and also contained some SMPs, but the aromatic protein-like substance was not obvious in the raw water. Furthermore, the hydrophobic fraction was mainly humic-like substances, and the hydrophilic fraction contained a small amount of organic matter with a low humification degree, and it also contains some protein-like organic matter.
- The decrease in specific flux caused by the HPO and N-HPI fractions was more serious, while the membrane fouling caused by the TPI and C-HPI fractions was lighter. Additionally, the HPO and N-HPI fractions were more likely to cause IF. From the fluorescent EEM spectra before and after membrane filtration, it can be found that humic-like substances and SMPs were the main foulants that caused IF, and a small amount of protein-like substances in the C-HPI fraction could also cause IF.
- The results of the Hermia model showed that the membrane fouling mechanism was mainly standard blocking and cake filtration during the test period, and the standard blocking had the highest fit among all fractions, with R^2 of 0.999 in the two-cycles.

Declaration of competing interest

The authors declare that they have no known competing financial interests or personal relationships that could have appeared to influence the work reported in this paper.

Acknowledgments

This research was supported by National Natural Science Fund (No: 51868019).

References

[1] W. Yu, T. Liu, J. Crawshaw, T. Liu, N. Graham, Ultrafiltration and nanofiltration membrane fouling by natural organic matter: mechanisms and mitigation by pre-ozonation and pH, Water Res., 139 (2018) 353–362.
[2] M. Schulz, A. Soltani, X. Zheng, M. Ernst, Effect of inorganic colloidal water constituents on combined low-pressure membrane fouling with natural organic matter (NOM), J. Membr. Sci., 507 (2016) 154–164.
[3] B.W. Ma, Y. Ding, W. Li, C. Hu, M. Yang, H. Liu, J. Qu, Ultrafiltration membrane fouling induced by humic acid with typical inorganic salts, Chemosphere, 197 (2018) 793–802.
[4] Y. Wan, P. Xie, Z. Wang, J. Ding, J. Wang, S. Wang, M.R. Wiesner, Comparative study on the pretreatment of algae-laden water by UV/persulfate, UV/chlorine, and UV/H_2O_2: variation of characteristics and alleviation of ultrafiltration membrane fouling, Water Res., 158 (2019) 213–226.
[5] X. Chen, J. Luo, B. Qi, W. Cao, Y. Wan, NOM fouling behavior during ultrafiltration: effect of membrane hydrophilicity, J. Water Process Eng., 7 (2015) 1–10.
[6] K. Li, F. Qu, H. Liang, S. Shao, Z. Han, H. Chang, X. Du, G. Li, Performance of mesoporous adsorbent resin and powdered activated carbon in mitigating ultrafiltration membrane fouling caused by algal extracellular organic matter, Desalination, 336 (2014) 129–137.
[7] X. Cheng, P. Li, W. Zhou, D. Wu, C. Luo, W. Liu, Z. Ren, H. Liang, Effect of peroxymonosulfate oxidation activated by powdered activated carbon for mitigating ultrafiltration membrane fouling caused by different natural organic matter fractions, Chemosphere, 221 (2019) 812–823.
[8] H. Yamamura, K. Okimoto, K. Kimura, Y. Watanabe, Hydrophilic fraction of natural organic matter causing irreversible fouling of microfiltration and ultrafiltration membranes, Water Res., 54 (2014) 123–136.
[9] L. Ao, W. Liu, L. Zhao, X. Wang, Membrane fouling in ultrafiltration of natural water after pretreatment to different extents, J. Environ. Sci., 43 (2016) 234–243.
[10] E. Zevenhuizen, V. Reed, S. Rahman, G. Gagnon, In-line coagulation to reduce high-pressure membrane fouling in an integrated membrane system: a case study, Desal. Water Treat., 56 (2015) 1987–1998.
[11] F. Qu, H. Liang, Z. Wang, H. Wang, H. Yu, G. Li, Ultrafiltration membrane fouling by extracellular organic matters (EOM) of *Microcystis aeruginosa* in stationary phase: influences of interfacial characteristics of foulants and fouling mechanisms, Water Res., 46 (2012) 1490–1500.
[12] A. Philippe, G.E. Schaumann, Interactions of dissolved organic matter with natural and engineered inorganic colloids: a review, Environ. Sci. Technol., 48 (2014) 8946–8962.
[13] J. Tian, C. Wu, H. Yu, S. Gao, G. Li, F. Cui, F. Qu, Applying ultraviolet/persulfate (UV/PS) pre-oxidation for controlling ultrafiltration membrane fouling by natural organic matter (NOM) in surface water, Water Res., 132 (2018) 190–199.
[14] J. Xing, H. Wang, X. Cheng, X. Tang, X. Luo, J. Wang, T. Wang, G. Li, H. Liang, Application of low-dosage UV/chlorine pre-oxidation for mitigating ultrafiltration (UF) membrane fouling in natural surface water treatment, Chem. Eng. J., 344 (2018) 62–70.
[15] K. Katsoufidou, S.G. Yiantsios, A.J. Karabelas, A study of ultrafiltration membrane fouling by humic acids and flux recovery by backwashing: experiments and modeling, J. Membr. Sci., 266 (2005) 40–50.

[16] K.S. Katsoufidou, D.C. Sioutopoulos, S.G. Yiantsios, A.J. Karabelas, UF membrane fouling by mixtures of humic acids and sodium alginate: fouling mechanisms and reversibility, Desalination, 264 (2010) 220–227.
[17] H.C. Kim, B.A. Dempsey, Membrane fouling due to alginate, SMP, EfOM, humic acid, and NOM, J. Membr. Sci., 428 (2013) 190–197.
[18] J.-Y. Tian, M. Ernst, F.Y. Cui, M. Jekel, Effect of different cations on UF membrane fouling by NOM fractions, Chem. Eng. J., 223 (2013) 547–555.
[19] H. Wang, A. Ding, Z. Gan, F. Qu, X. Cheng, L. Bai, S. Guo, G. Li, H. Liang, Fluorescent natural organic matter responsible for ultrafiltration membrane fouling: fate, contributions and fouling mechanisms, Chemosphere, 182 (2017) 183–193.
[20] J. Fan, T. Lin, W. Chen, H. Xu, H. Tao, Control of ultrafiltration membrane fouling during the recycling of sludge water based on Fe(II)-activated peroxymonosulfate pretreatment, Chemosphere, 246 (2020) 125840, doi: 10.1016/j.chemosphere.2020.125840.
[21] X. Wang, M. Zhou, X. Meng, L. Wang, D. Huang, Effect of protein on PVDF ultrafiltration membrane fouling behavior under different pH conditions: interface adhesion force and XDLVO theory analysis, Front. Environ. Sci. Eng., 10 (2016) 12, doi: 10.1007/s11783-016-0855-9.
[22] Z. Liu, H. Chu, B. Dong, H. Liu, Characterization of natural organic foulants removed by microfiltration, Desalination, 277 (2011) 370–376.
[23] X. Meng, W. Tang, L. Wang, X. Wang, D. Huang, H. Chen, N. Zhang, Mechanism analysis of membrane fouling behavior by humic acid using atomic force microscopy: effect of solution pH and hydrophilicity of PVDF ultrafiltration membrane interface, J. Membr. Sci., 40 (2015) 180–188.
[24] S. Völker, C. Schreiber, T. Kistemann, Drinking water quality in household supply infrastructure—a survey of the current situation in Germany, Int. J. Hyg. Environ. Health, 213 (2010) 204–209.
[25] C. Jacquin, N. Gambier, G. Lesage, M. Heran, New insight into fate and fouling behavior of bulk dissolved organic matter (DOM) in a full-scale membrane bioreactor for domestic wastewater treatment, J. Water Process Eng., 22 (2018) 94–102.
[26] Y.H. Teow, Z.H. Wong, M.S. Takriff, A.W. Mohammad, Fouling behaviours of two stages microalgae/membrane filtration system applied to palm oil mill effluent treatment, Membr. Water Treat., 9 (2018) 373–383.
[27] W. Zhang, L. Ding, N. Grimi, M.Y. Jaffrin, B. Tang, A rotating disk ultrafiltration process for recycling alfalfa wastewater, Sep. Purif. Technol., 188 (2017) 476–484.
[28] S. Wong, J.V. Hanna, S. King, T.J. Carroll, R.J. Eldridge, D.R. Dixon, B.A. Bolto, S. Hesse, G. Abbt-Braun, F.H. Frimmel, Fractionation of natural organic matter in drinking water and characterization by 13C cross-polarization magic-angle spinning NMR spectroscopy and size exclusion chromatography, Environ. Sci. Technol., 36 (2002) 3497–3503.
[29] M. Kawahigashi, H. Sumida, K. Yamamoto, Size and shape of soil humic acids estimated by viscosity and molecular weight, J. Colloid Interface Sci., 284 (2005) 463–469.
[30] V.P. Irina, H.F. Fritz, V.K. Dmitrii, A. Gudrun, V.K. Alexey, H. Sebastian, Development of a predictive model for calculation of molecular weight of humic substance, Water Res., 32 (1998) 872–881.
[31] W. Chen, P. Westerhoff, J.A. Leenheer, K. Booksh, Fluorescence excitation-emission matrix regional integration to quantify spectra for dissolved organic matter, Environ. Sci. Technol., 37 (2015) 5701–5710.
[32] Y. Shen, W. Zhao, X. Kang, X. Huang, A systematic insight into fouling propensity of soluble microbial products in membrane bioreactors based on hydrophobic interaction and size exclusion, J. Membr. Sci., 346 (2010) 187–193.
[33] S.A. Huber, F.H. Frimmel, Direct gel chromatographic characterization and quantification of marine dissolved organic carbon using high-sensitivity DOC detection, Environ. Sci. Technol., 28 (1994) 1194–1197.
[34] H. Namguk, A. Gary, M. Diane, S. Jinsik, Y. Yeomin, Characterization of DOM as a function of MW by fluorescence EEM and HPLC-SEC using UVA, DOC, and fluorescence detection, Water Res., 37 (2003) 4295–4303.
[35] H. Yamamura, K. Kimura, Y. Watanabe, Mechanism involved in the evolution of physically irreversible fouling in microfiltration and ultrafiltration membranes used for drinking water treatment, Environ. Sci. Technol., 41 (2007) 6789–6794.
[36] N. Kawasaki, K. Matsushige, K. Komatsu, A. Kohzu, F.W. Nara, F. Ogishi, M. Yahata, H. Mikami, T. Goto, A. Imai, Fast and precise method for HPLC–size exclusion chromatography with UV and TOC (NDIR) detection: importance of multiple detectors to evaluate the characteristics of dissolved organic matter, Water Res., 45 (2011) 6240–6248.
[37] J. Guo, H. Liu, J.H. Liu, L.Y. Wang, Ultrafiltration performance of EfOM and NOM under different MWCO membranes: Comparison with fluorescence spectroscopy and gel filtration chromatography, Desalination, 344 (2014) 129–136.
[38] R.K. Henderson, A. Baker, K.R. Murphy, A. Hambly, R.M. Stuetz, S.J. Khan, Fluorescence as a potential monitoring tool for recycled water systems: A review, Water Res., 43 (2009) 863–881.
[39] H. Naomi, B. Andy, R. Darren, Fluorescence analysis of dissolved organic matter in natural, waste and polluted waters—a review, River Res. Appl., 23 (2007) 631–649.
[40] F.C. Wu, R.D. Evans, P.J. Dillon, Separation and characterization of NOM by high-performance liquid chromatography and on-line three-dimensional excitation emission matrix fluorescence detection, Environ. Sci. Technol., 37 (2003) 3687–3693.
[41] T. Zhang, J. Lu, J. Ma, Z. Qiang, Fluorescence spectroscopic characterization of DOM fractions isolated from a filtered river water after ozonation and catalytic ozonation, Chemosphere, 71 (2008) 911–921.
[42] J. Swietlik, E. Sikorska, Application of fluorescence spectroscopy in the studies of natural organic matter fractions reactivity with chlorine dioxide and ozone, Water Res., 38 (2004) 3791–3799.
[43] N. Senesi, Molecular and quantitative aspects of the chemistry of fulvic acid and its interactions with metal ions and organic chemicals: Part I. The electron spin resonance approach, Anal. Chim. Acta, 232 (1990) 51–75.
[44] L. Fan, J.L. Harris, F.A. Roddick, N.A. Booker, Influence of the characteristics of natural organic matter on the fouling of microfiltration membranes, Water Res., 35 (2001) 4455–4463.
[45] W. Sun, J. Nan, X. Jia, J. Tian, Identifying the major fluorescent components responsible for ultrafiltration membrane fouling in different water sources, J. Environ. Sci., 45 (2016) 215–223.
[46] W. Sun, J. Nan, X. Jia, J. Tian, The influence and the mechanism of different molecular weight organic in natural water to the ultrafiltration membrane fouling reversibility, RSC Adv., 86 (2016) 83456–83465.
[47] Z. Wang, Y. Wan, P. Xie, A. Zhou, J. Ding, J. Wang, L. Zhang, S. Wang, T.C. Zhang, Ultraviolet/persulfate (UV/PS) pretreatment of typical natural organic matter (NOM): variation of characteristics and control of membrane fouling, Chemosphere, 214 (2019) 136–147.
[48] R. Miao, X. Li, W. Ying, P. Wang, L. Wang, G. Wu, J. Wang, Y. Lv, T. Liu, A comparison of the roles of Ca^{2+} and Mg^{2+} on membrane fouling with humic acid: are there any differences or similarities, J. Membr. Sci., 545 (2017) 81–87.
[49] V.L. Quang, H.-C. Kim, T. Maqbool, J. Hur, Fate and fouling characteristics of fluorescent dissolved organic matter in ultrafiltration of terrestrial humic substances, Chemosphere, 165 (2016) 126–133.
[50] B.W. Ma, G.Z. Wu, W.J. Li, R. Miao, X.F. Li, P. Wang, Roles of membrane–foulant and inter/intrafoulant species interaction forces in combined fouling of an ultrafiltration membrane, Sci. Total Environ., 652 (2019) 19–26.
[51] K. Katsuki, H. Yasushi, W. Yoshimasa, A. Gary, O. Naoki, Irreversible membrane fouling during ultrafiltration of surface water, Water Res., 38 (2004) 3431–3441.

[52] H. Namguk, A. Gary, C. Jinwook, Y. Jaekyung, Y. Yeomin, Characterizing dissolved organic matter and evaluating associated nanofiltration membrane fouling, Chemosphere, 70 (2008) 495–502.
[53] S. Zhou, Y. Shao, N. Gao, Y. Deng, L. Li, J. Deng, C. Tan, Characterization of algal organic matters of *Microcystis aeruginosa*: biodegradability, DBP formation and membrane fouling potential, Water Res., 52 (2014) 199–207.
[54] L. NoHwa, A. Gary, C. Jean-Philippe, B. Herve, Identification and understanding of fouling in low-pressure membrane (MF/UF) filtration by natural organic matter (NOM), Water Res., 38 (2004) 4511–4523.